論 文

다중파 전파전파환경에서의 이동화상통신의 동기시간 변동량해석에 관한 연구

正會員 河 德 鎬*

An Analysis of the SYNC Timing Fluctuations in Mobile Visual Communicatuion Under Urban Multipath Propagation Environments

Deock Ho HA* *Regular Member*

要 約   광대역 화상정보신호(TV방송파)의 이동수신에 의한 화상품질열화는 고정수신의 경우와는 전혀 다른 상황을 나타내며, 이동체의 이동과 더불어 시시각각 복잡하게 변화한다. 본 논문에서는 야외 및 실내에서의 기초적 실험에 의해 텔레비 이동수신에서 Fluttering ghost가 화상품질열화원인중 가장 중요하다고 생각하여, 그 발생원인과 특성을 조사했다. Fluttering ghost는 텔레비 수상기에서 재생되는 수평동기펄스의 동기시각이 다중파간섭 페이딩에의해 불안정하게 변동하므로서 발생한다는 것을 알았다. 따라서 H-sync pulse timing의 다중파 조건에 대한 변화를 이론적으로 해석하고 그 특성을 밝혀 동기시간변동의 조건과 원인을 밝혔다.

ABSTRACT   This paper represents the occurrence structure of the timing variation of TV horizontal synchronizing pulse(H-sync pulse) in mobile TV reception. Fluttering ghost is caused by timing variations of the H-sync pulse and is due to frequency selective fading in a multipath propagation environment. H-sync timing fluctuations, and hence, fluttering ghost are directly correlated with the multipath parameters, i.e., H-sync timing fluctuations reflect well the severity of the multipath environment. The occurrence structure of H-sync timing fluctuation is analysed theoretically in relation to the multipath parameters, assuming the two-ray propagation model. The H-sync timing fluctuation occurs with the variation in relative phase and/or D/U variation of long-delayed multipath waves.

Ⅰ. Introduction

*國立釜山水産大學 電子工學科
Dept. of Electronic Engineering, National Fisheries University of Pusan, Pusan, Korea.
論文番號：89-46(接受 1989. 4. 28)

Picture quality in mobile TV reception is much worse than that in primary fixed reception in urban areas. The results of both field observation and laboratory simulation indicate that fluttering ghost is the most severe picture

472

impairment among various kinds of picture impairment. [1]

This paper is concerned with phenomena herein called "fluttering ghost", which is the simultaneous occurrence of the two separate phenomena of ghost images and fluttering, i.e., the appearance of ghost images which flutter rapidly to and for across the TV screen. It is established that fluttering ghost results from H-sync timing fluctuations. In stationary TV reception, ghost images results from excess time delays. Delays of 1 microsecond or more are common in urban areas[2]. When receiving a TV signal while in motion in an urban area, these excess time delays lead to ghost images which flutter. The effect of the excess time delays are reflected in fluctuating H-sync timing delays.

Simulation of the two-ray model in the laboratory reproduces fluttering ghost as it is actually observed in the field. It will be shown in this paper that fluttering ghost is due to fluctuations in the time delay of the H-sync pulse.

Laboratory simulation tests, assuming the Rayleigh-distributed two-ray model, can display the general characteristics of fluttering ghost. Relations between multipath parameters(mean signal strength, delay time, DU ratio and RF phase differece) and the fluctuation of H-sync pulse timing are analysed. The results of the analysis show how fluttering ghost is caused in relation to the multipath parameters. It is clearly seen that the fluttering ghost represented by H-sync timing fluctuation in very much dependent on multipath propagation.

The structure of H-sync timing fluctuations can be theoretically analysed using multipath propagtion models, and measured in the field or laboratory using a model of two stationary rays with rotating relative phase.

II. Fundamental considerations on Picture Impairments.

There are many impairments in picture quality, many of which are affected by multipath propagation in urban areas. Some of the problems which appear in urban mobile TV reception are: snow noise, lack of clear and sharp image, variation in purity and density of color, appearance of ghost images, and flutter of an image on the screen, and so on. Some take place soley, but in many cases more than two appear simultaneously. Ghost images are common, and usually flutter to and fro rapidly, resulting in the phenomenon called fluttering ghost in this paper. It is not easy to separate each impairment in a dynamically changing picture. According to the observations, however, loss of sync and fluttering ghost seem to be the most serious impairments.

Certain features of picture impairment in urban areas can be reproduced in the laboratory by use of a signal transmission channel simulating the multipath propagation. To analyze multipath interference effects, a single ray, stationary two-ray, and Rayleigh-distributed two-ray propagation models were considered. Figure 1 shows a schematic diagram of the configuration used in the laboratory simulation. A two-ray multipath fadingis is simulated using a Rayleigh-fading simulator, attenuators to vary the DU ratio, and a delay line and a phase shifter inserted in the U-wave and D-wave channels to vary delay time and phase difference (the first incoming signal is denoted hereafter by "Desired"or D-wave, and the delayed signal denoted by "Undesired" or U-wave).

II-1 Test on Single-ray Model
A single-ray model is simulated by deleting
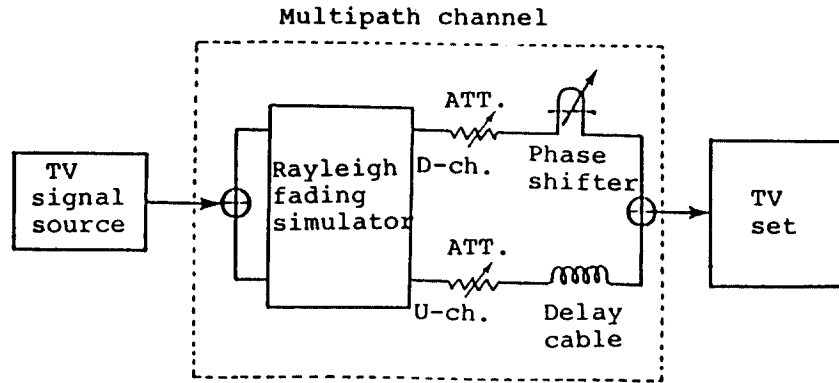
473

Multipath channel

Fig.1 Schematic diagram of Rayleigh-distributed two-ray model.

the U-channel in the Figure 1. The signal level fluctuates subject to the Rayleigh distribution without multipath delays.

It was observed that the resulting SNR degradation due to fading does not generate the severe impairments as generally observed in mobile TV reception in urban areas, but instead causes simple snow noise and occasional loss of sync response to very deep fade.

II-2 Test on Stationary Two-ray Model

In this model two rays are considered but the vehicle is assumed stationary (i.e., Fixed TV reception is simulated). The fading sim-ulator is disconnected and the DU ratio and relative phase are varied manually.

In this configuration, loss of sync and var-iations of purity and/or density of color are observed when a frequency-selective deep fade takes place in the vicinity of the carrier fre-quency or color subcarrier frequency. Figure 2 shows an example of the power spectrum of a composite video signal in the case of loss of sync. When the sync signal power is lost because of deep fade, loss of sync is observed.

By changing the DU ratios, delay line or phase difference, ghost images can be repro-
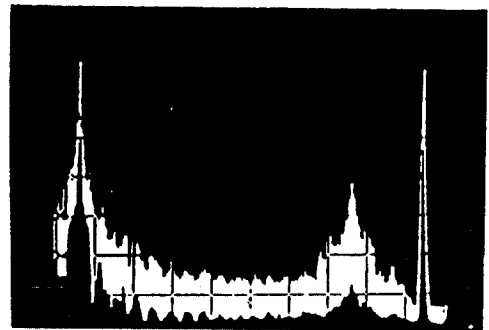
(a)

(b)

(c)

Fig.2. RE spectrum of TV signal in multipath propagation:
(a) normal spectrum;
(b) spectrum with multipath fading;
(c) frequency selectivity of multipath channel.

474

duced. Ghost images can be most clearly seen in the case where the DU ratio is near zero decibel and a longer delay line is inserted. Ghost images appear to the right or left on the screen by changing DU ratio and phase difference.

II-3 Test on Rayleigh-distributed Two-ray Model

Two Rayleigh-distributed rays of random phase difference are interfered with each other in this simulation. The TV pictures observed display impairment almost indentical to that experienced in the actual mobile reception in an urban area, i.e., display fluttering ghost.

The fluttering ghost on the screen varies dynamically in accordance with the signal fading, because both the DU ratio of the two rays and relative phase are varied by a Rayleigh fading simulator. Furthermore, the severity of fluttering ghost increases as the delay line is lengthened.

From the laboratory simulations mentioned above it can be concluded that loss of sync is caused by a frequency-selective deep fade, and that fluttering ghost occurs due to phase changes and / or the variations in the DU ratio of the long-delayed multipath waves.

III. Representation of Fluttering Ghost by Means of H-sync Pulse Timing

Fluttering ghost can be detected by measuring the fluctuations of H-sync pulse timing. Now consider how H-sync pulse timing is affected by multipath fading with long delay time.

The synchronizing pulse, generally called sync pulse, is a part of the composite video signal and is the hightest 25 percent of the signal amplitude. Included in it are the horizontal, vertical, and equalizing pulses. These are clipped from the video signal by the sync separator. The sync pulse is then coupled to the horizontal and vertical deflection oscillators to time the scanning freqencies. The TV picture can then be correctly reproduced on the screen. H-sync pulses hold the line structure of the picture together by locking in on the frequency of the horizontal oscillator. But, if the H-sync timing fluctuates, then the picture also fluctuates on the screen.

Horizontal deviation of the picture is therefore related to the H-sync timing. If the H-sync pulse is regenerated incorrectly, the received picture is not correctly reproduced horizontally in step with that of the transmitted picture. In the case of fixed point TV reception the H-sync pulse is in a steady-state H-sync pulse and hence a satisfactory picture is always reproduced.

But, in the case where a signal is received by a vehicle in motion through a multipath interference patten, the composite video signal is dynamically distorted by frequency-selective fading. Hence, the H-sync pulse, when separated from a dynamically distorted composite video signal in the TV receiver, varies in timing compared to the reference timing.

Multiple delayed waves cause multiple ghost images in urban fixed TV reception. In urban mobile TV reception the H-sync timing fluctuates in a complex manner, as the signal suffers from more complicated distortion. As will be shown in this paper the variations in the H-sync timing are dependent on the multipath parameters such as DU ratio and relative phase difference.
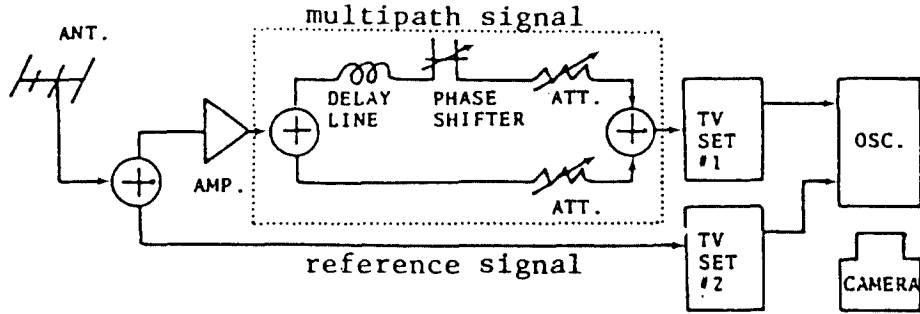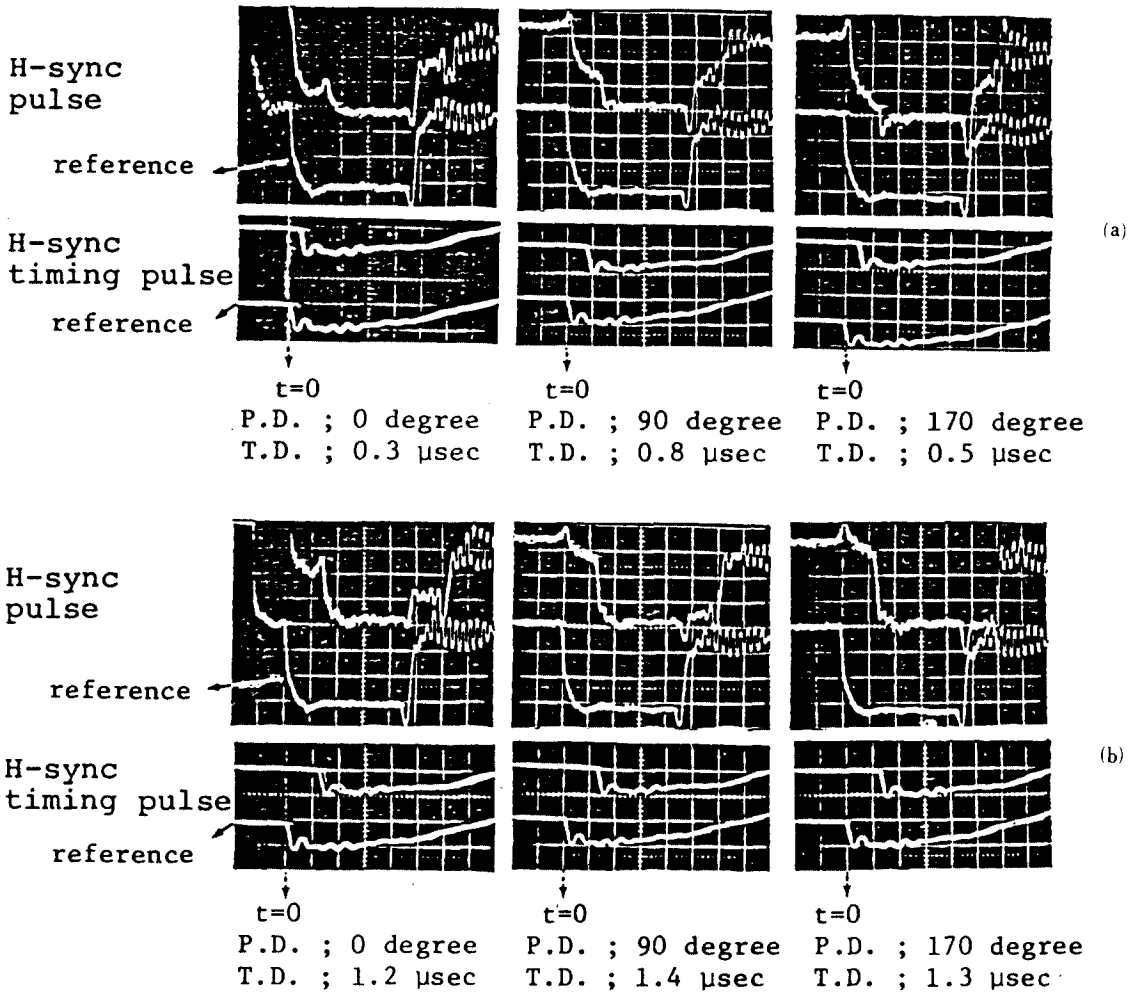
IV. Simulation of Fluttering Ghost

475

Fig.3 Measuring system for stationary Two-ray model.

H-sync
pulse

reference

H-sync
timing pulse

reference

(a)

t=0   t=0   t=0
P.D. ; 0 degree   P.D. ; 90 degree   P.D. ; 170 degree
T.D. ; 0.3 μsec   T.D. ; 0.8 μsec   T.D. ; 0.5 μsec

H-sync
pulse

reference

H-sync
timing pulse

reference

(b)

t=0   t=0   t=0
P.D. ; 0 degree   P.D. ; 90 degree   P.D. ; 170 degree
T.D. ; 1.2 μsec   T.D. ; 1.4 μsec   T.D. ; 1.3 μsec

P.D.=phase difference, T.D.=timing deviation
(Lateral scale : 1 μsec/div)

Fig.4 H-sync pulse distortions for various multipath para-
meters: (a) DU ratio 5dE, excess time delay 1.3μsec;
(b) DU ratio -5dB, excess time delay 1.3μsec.

476

In order to investigate the relationship bet-ween H-sync timing and multipath parameters (DU ratio and phase difference), first a labo ratory simulation of the stationary two ray model(i.e., urban fixed TV reception) was conducted. This test system is showen in Figure 3. In this case, the delay line is set at a value of 1.3 microseconds. By varying the DU ratio and the relative phase difference, changes in the H sync pulse waveform can be observed by comparing it to a reference (transmitted) waveform.

Figure 4 shows comparisons of the distorted and the reference H sync pulses received by TV sets, and the H-sync pulses regenerated within the TV set, herein called "H sync timing pulses". Each of the lower waveforms in the figure represents the reference wavef-orm. The distorted H sync pulse waveform varies with reference waveform. The distorted H-sync pulse waveform varies with different values of the DU ratio and relative phase difference, and shows a shift to the right relative to the reference time t=0. The timing of the H-sync pulse can be set at any specific level in the H sync separator in the TV rec-eiver. In this case, it is set at 70 percent of the maximum amplitude of H-sync waveform.

A preliminary field test was made to observe the timing variation of the regenerated H-sync pulse when a vehicle in motion in an urban area received a TV signal. With the measuring system by removing the part of multipath signal as shown in Figure 3, the field test was carried out on the campus of Kyoto University, where it was clear that two principal rays existed as shown in Figure 5(a). In this test course it was ascertained by the directional pattern measured by a directive antenna that a diffracted wave arriving from the southerly direction and a wave reflected from a building arriving from the northerly existed[a].

The TV broadcast signal (VHF 12ch.; picture carrier frequency 205.25MHz) were received by an omni-directional antenna (turn stile antenna; Gain 1.9dB) mounted on the roof top(about 3m above the ground) of a mobile laboratory. As a reference signal, the signal received by a fixed directive antenna (Gain 4dB, front-to-back ratio 14~17dB, half-power beamwidth 65 degrees) mounted on top of a near by building was used. The difference of H-sync pulse timing between the measured and the reference was converted into the value relative to free space, i.e., the physical distance between the reference ante nna and measuring antenna including the length of the antenna feeder was compensated.

H = Building height (meters)

(a)

→ reference

(Lateral scale :
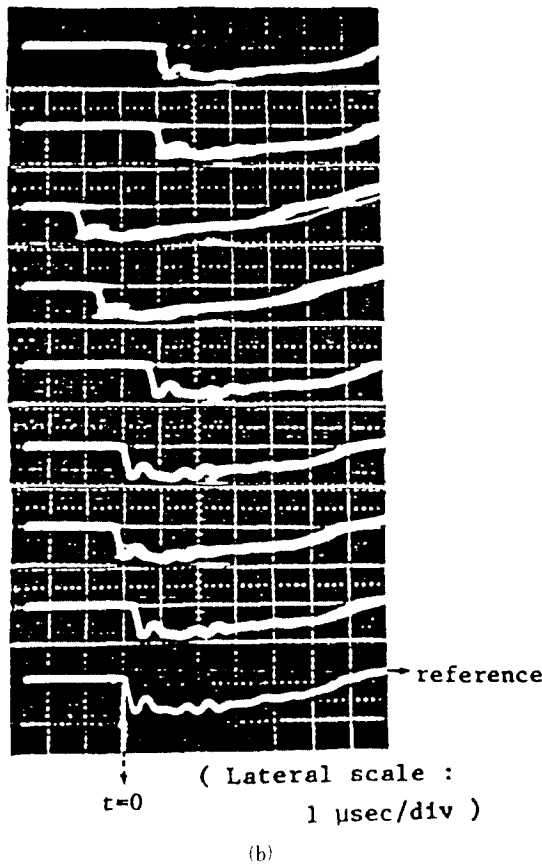t=0   1 μsec/div)

(b)
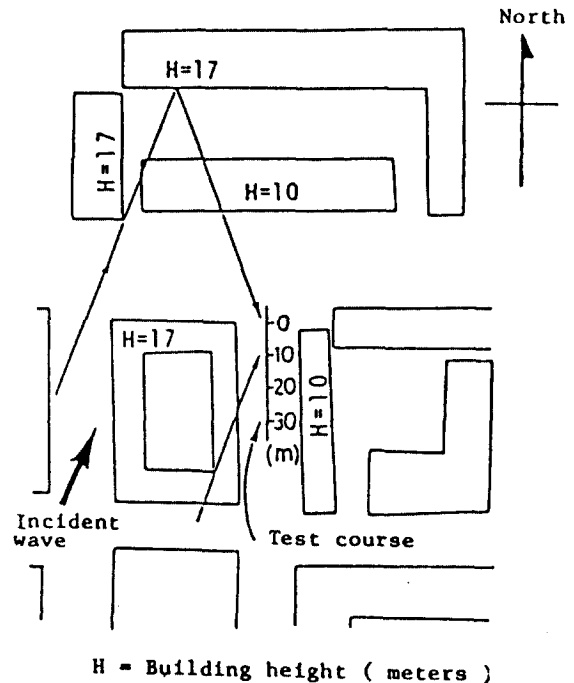
Fig.5 (a) Preliminary field test course,
       (b) H-sync timing variation in a field test.

The photograph of measuring H-sync timing pulse from the TV set ♯1 was taken by a vehicle in stop with a 5 meter interval Figure 5(b) shows the measured H-sync timing pulse in the field test. The waveform at the bottom of the figure is a· reference H-sync timing pulse. The observed H-sync timing pulse varies with the test point. It means that the timing pulse varies with the vehicle motion. The signals taking a faster timing than the reference signal in the figure indicate the turbulence caused by an unstable synchronization. Also, the appearance of fluctuating ghost images and loss of sync were simultaneously observed

on the TV screen. It can be concluded therefore that when a TV signal is received in a moving vehicle in an urban area the H-sync timing varies dynamically resulting in fluttering ghost.

Ⅴ. Theoretical Analysis of Fluttering Ghost

Ⅴ-1 H-sync Pulse Waveform in Two-ray model

For simplicity, consider only the H-sync pulse which is included in the RF composite video signal, and assume the two-ray propagation model. The regenerated H-sync pulse in the TV receiver (H-sync timing pulse) is simulated as shown in Figure 6. The resultant waveform of two amplitude-modulated signals is detected by the video detector. The magnitudes of these waveforms are restricted to a constant level by the AGC circuit. The H-sync pulse is clipped by the cutoff level of sync-separator circuit. Hence, "new" H-sync timing pulses, whose timing is determined by the cutoff characteristics of the sync-separator, are regenerated in the TV receiver.

The resultant waveform resulting from interference of the D-and U-waves is distorted. Therefore, the regenerated H-sync timing pulses take on many timing values depending on the multipath parameters, and thus fluttering ghost occurs.

Ⅴ-2 Analysis of Timing Conditions of Resultant H-sync Pulse

If the influence of the Nyquist filtering and envelope detection operations on the composite video signal are ignored, the H-sync timing pulse characteristics in a two-ray propagation model can be easily analysed.
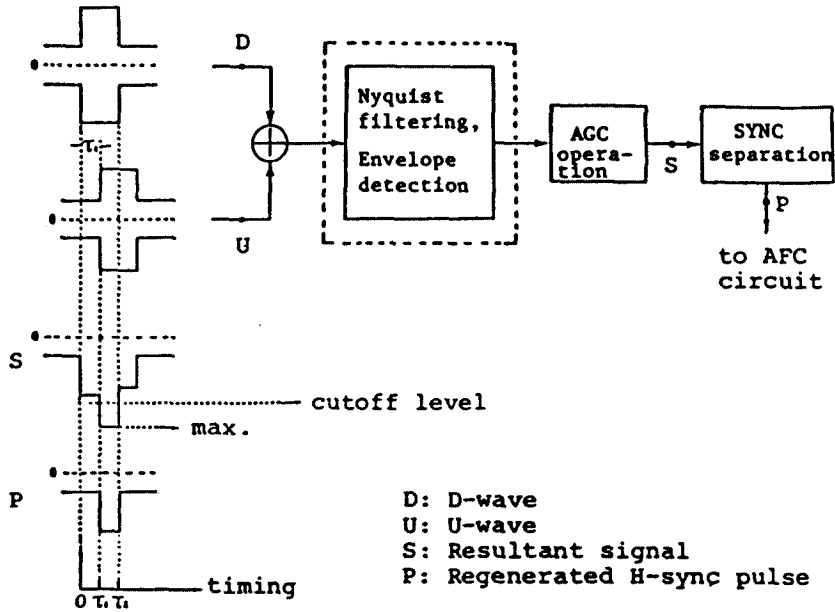
478

Fig.6 Diagram of regenerated horizontal sync pulse.

Two ray signals (D-wave and U-wave) for the two-ray propagation model can le expressed in the form

$$\text{D-wave; } e_d(t) = E_d \cdot \exp(j\,\omega_c t) \qquad (1)$$

$$\text{U-wave; } e_u(t) = E_u \cdot \exp[j(\omega_c(t - \tau_1) - \phi)] \qquad (2)$$

where E_d is the amplitude of D-wave, E_u is the amplitude of U-wave, ω_c is the angular frequency of the carrier signal, τ_1 is the propagation delay of U-wave relative to D-wave and ϕ is the phase difference between the U-and D-waves. The waveform of a resultant H-sync pulse before entering the detection is shown in Figure 7.

The amplitude ratio, ρ, of the two waves and a DU ratio can be defined as follows:

$$\rho = \begin{pmatrix} E_u / E_d \;\; (E_d \geqq E_u) \\ E_d / E_{u'} \;\; (E_d < E_u), \end{pmatrix} \qquad (3)$$

$$0 \leqq \rho \leqq 1,$$

$$\text{DU ratio} = \begin{pmatrix} 20 \cdot \log(1/\rho), \;\; (E_d \geqq E_u) \\ -20 \cdot \log(1/\rho), \;\; (E_d < E_u). \end{pmatrix} \qquad (5)$$

The amplitude E_r of the resultant waveform of the two waves can be expresed as follows:

$$E_r = \sqrt{E_d^2 + 2E_d \cdot E_u \cos\psi + E_u^2}, \qquad (6)$$

where, $\psi = \omega_c \tau_1 + \phi$, $\;\; 0 \leqq \psi \leqq \pi$.

As shown in Figure 7, the resultant H-sync pulse has three sections, called A, B, and C in the figure. Region A is the time interval in which the amplitude has the value E_d,

479

region B, the time interval of amplitude E_r, and region C that of E_u.

As mentioned above, the H-sync waveform is controlled by AGC circuit. Therefore, the waveform is normalized to the maximum value among the three amplitudes E_d, E_r, E_u.

Let the H-synce separator's cutoff level normalized to the maximum value of pulse amplitude be $\alpha(0.5 \leq \alpha \leq 1)$, then the timing of the regenerated H-sync pulse is determined by the time that the waveform first exceeds the value α. Therefore, the synchronous timing of the H-sync pulse will take on a value of 0, τ_1, or τ_2 depending on the shape of the resultant waveform. The Table 1 shows the classification of possible timing conditions. The timing conditions formulas are derived in the next section.
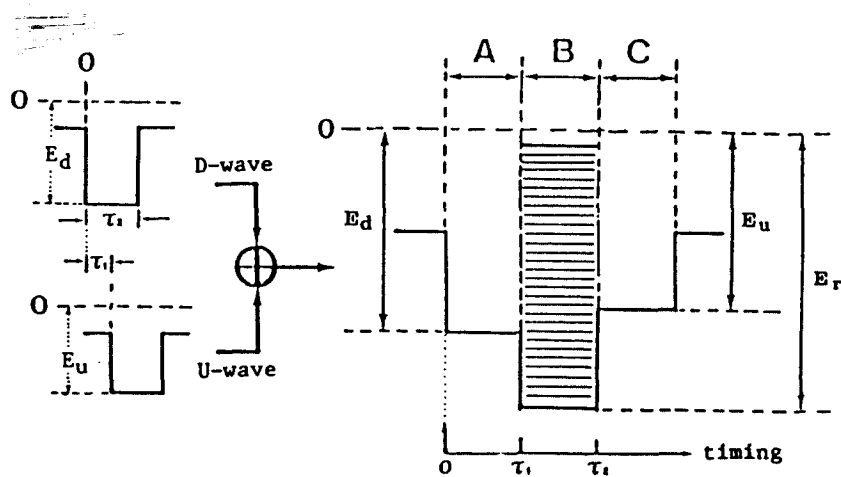

Fig.7 Example of resultant horizontal sync pulse.

V-3 Timing Condition Formulas

First, consider the case $E_d \geq E_u$ in Table 1. The synchronizing time has a value of 0 or τ_1.

(Case I.)

When E_d is greater than E_r then:

$$E_r / E_d \langle 1 \qquad (7)$$

The synchronizing time always has the value of 0. Using Eq.(6) this condition yields the following:

$$\rho^2 + 2\rho \cdot \cos \Psi \langle 0 \cdot \qquad (8)$$

The phase condition which results is:

$$\cos^{-1}(-\rho / 2) \langle \Psi \leq \pi \qquad (9)$$

Because the phase Ψ, by definition, is restricted to the range $0 \leq \Psi \leq \pi$, the value ρ can take on only values between -2 and 2. But, again by definition, ρ is restricted to the range $0 \leq \rho \leq 1$.

Therefore, when the phase Ψ fulfills the conditions of Eq.(9), the timing is always 0, regardless of the value of ρ.

(Case II.)

When E_r is greater than E_d and synchronizing time is 0, then:

480

Table.1 Normalized resultant horizontal sync pulses and timing conditions.

	Maximum amplitude	Cutoff conditions	Normalized resultant waveforms	Timing	Timing condition formulas
$E_d \geqq E_u$	E_d	$E_d > E_r$		0	$0 \leqq \rho \leqq 1$ $\cos^{-1}(-\rho/2) < \Psi \leqq \pi$
	E_r	$E_d > \alpha$ $E_d/E_r > \alpha$		0	$\dfrac{(1-\alpha)}{\alpha} \leqq \rho \leqq 1$ $\cos^{-1}\left(\dfrac{(1/\alpha^2-1)-\rho^2}{2\rho}\right) < \Psi < \cos^{-1}\left(\dfrac{-\rho}{2}\right)$
	E_r	$E_d < \alpha$ $E_d/E_r < \alpha$		r_1	$\dfrac{(1-\alpha)}{\alpha} \leqq \rho \leqq 1$ $0 \leqq \Psi < \cos^{-1}\left(\dfrac{(1/\alpha^2-1)-\rho^2}{2\rho}\right)$
$E_d < E_u$	E_r	$E_d > \alpha$ $E_d/E_r > \alpha$		0	$\alpha \leqq \rho \leqq 1$ $\cos^{-1}\left(\dfrac{(1/\alpha^2-1)\cdot\rho^2-1}{2\rho}\right) < \Psi < \cos^{-1}\left(\dfrac{-\rho}{2}\right)$
	E_r	$E_d < \alpha$ $E_d/E_r < \alpha$		r_1	$\alpha \leqq \rho \leqq 1$ $0 \leqq \Psi < \cos^{-1}\left(\dfrac{(1/\alpha^2-1)\cdot\rho^2-1}{2\rho}\right)$
	E_u	$E_d > \alpha$ $E_d/E_u > \alpha$		0	$\alpha \leqq \rho \leqq 1$ $\cos^{-1}\left(\dfrac{-\rho}{2}\right) < \Psi \leqq \pi$
	E_u	$E_d < \alpha$, and $E_r > \alpha$ $E_d/E_u < \alpha$ $E_r/E_u > \alpha$		r_1	$(1-\alpha) \leqq \rho < \alpha$ $0 \leqq \Psi < \cos^{-1}\left(\dfrac{(\alpha^2-1)-\rho^2}{2\rho}\right)$
	E_u	$E_d < \alpha$, and $E_r < \alpha$ $E_d/E_u < \alpha$ $E_r/E_u < \alpha$		r_1	$(1-\alpha) \leqq \rho < \alpha$ $\cos^{-1}\left(\dfrac{(\alpha^2-1)-\rho^2}{2\rho}\right) < \Psi \leqq \pi$

$$E_r > E_d, \qquad (10)$$

$$E_d / E_r > \alpha. \qquad (11)$$

Substituting Eq.(10) into Eq.(6) gives:

$$\Psi < \cos^{-1}(-\rho/2), \qquad (12)$$

and substituting Eq.(11) into Eq.(6) gives:

$$\Psi > \cos^{-1}\left[((1/\alpha^2-1)-\rho^2)/2\rho\right] \qquad (13)$$

Hence, from Eq.(12) and Eq.(13), the following phase condition is obtained:

$$\cos^{-1}\left[((1/\alpha^2-1)-\rho^2)/2\rho\right] < \Psi < \cos^{-1}(-\rho/2). \qquad (14)$$

Because the phase Ψ, by definition, is restricted to the range $0 \leqq \Psi \leqq \pi$, the following amplitude condition formula is obtained. First, from Eq.(4) and Eq.(12),

481

$$0 \leq \rho \leq 1. \qquad (15)$$

and second from Eq.(13),

$$[(1 / \alpha^2 - 1) - \rho^2] / 2\rho \leq 1, \qquad (16)$$

$$[(1 / \alpha^2 - 1) - \rho^2] / 2\rho \leq -1, \qquad (17)$$

Hence, the amplitude condition formula that fulfills simultaneously Eq.(15), Eq.(16) and E q.(17) can be expressed as follows:

$$(1 / \alpha) / \alpha \leq \rho \leq 1. \qquad (18)$$

(Case Ⅲ.)

When the synchronizing time is τ_1, then, the amplitude relation is given as follows:

$$E_d / E_r \langle \alpha. \qquad (19)$$

$$E_r \rangle E_d. \qquad (20)$$

Applying the same method as in Case I to Eq.(19) and Eq.(20), the following amplitude and phase condition formulas are obtained:

$$(1 - \alpha) / \alpha \leq \rho \leq 1. \qquad (21)$$

$$0 \leq \Psi \langle \cos^{-1}[((1 / \alpha^2 - 1) - \rho^2) / 2\rho]. \qquad (22)$$

This completes the derivation of the condition formulas for the case of $E_d \geq E_u$.

Similar to the preceding analysis, the formulas ca also be obtained for the case of $E_d \rangle E_u$. Thus, it has been demonstrated how the timing condition formulas of Table 1 are derived.

V-4 Relationship between H-sync Timing and Multipath Parameters

Assuming the relative time delay of the two rays is constant and DU ratio and phase difference are varied, the characteristics of the H-sync timing pulse can be examined. It is easy to express on the graph the timing condition formulas of Table 1.

Figure 8 shows the region where the H-sync timing, with the cutoff level α as a parameter, takes the values of 0, τ_1, or τ_2, in accordance with the variation of the DU ratio and phase difference. When the DU ratio is greater tha $20\log[\alpha / (1 - \alpha)]$, the synchronizing time always has the value 0. when the DU ratio is less than this value and phase difference is small, the TV receiver synchronizes with the U-wave and the synchronizing time is τ_1. When the DU ratio is between $-20\log(1 / \alpha)$ and $-20\log$
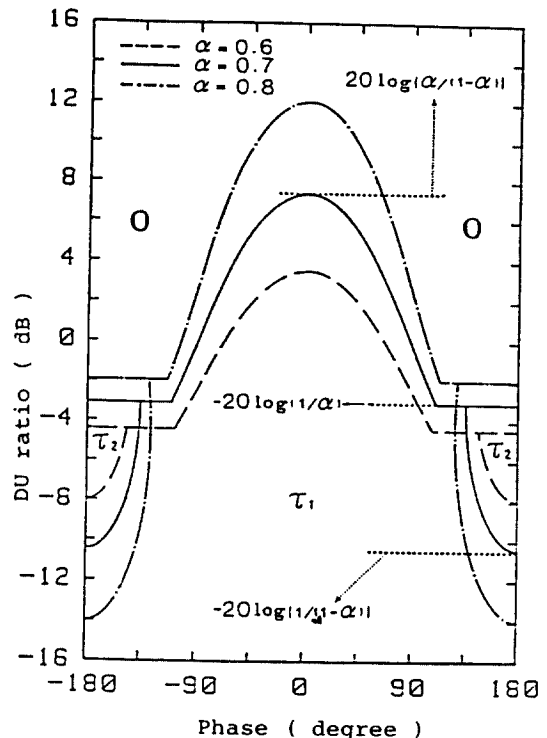

Fig.8 Timing regions for various values of phase difference and DU ratios.

$[1 / (1-\alpha)]$, the synchronizing time is τ_2. for the phase difference in the vicinity of ± 180 degrees. and τ_1 for the phase differences not in the vicinity of ± 180 degrees. In the case where the DU ratio is less than the value - $20\log[1/(1-\alpha)]$, the synchronizing time always takes the value of τ_1, irrespective of the phase difference, because the TV receiver synchronizes with the U-wave. The lower the cutoff level the more often the synchronizing time 0, and the less often τ_2.

In general, as previously stated, the H-sync timing varies in the each region in accordance with the value of the multipath parameters, as shown in figure 8. In order to examine the relation between the H-sync timing and received-signal strength (amplitude of resultant waveform), the DU ratio is held constant (e.g. 3dB, -3dB, -6dB) and only the phase is varied. This is shown is Figure 9, where $\alpha=0.7$, A correspondence between signal strength and H-sync timing can be seen, i.e., their fades are similar when the DU ratio is between $20\log[\alpha/(1-\alpha)]$ and $-20\log(1/\alpha)$ as shown in Figure 9(a), (b). When the DU ratio is less than $-20\log(1/\alpha)$ the fades are opposite, shown in Figure 9(c).

Also, the case of two stationary rays of constant DU ratio and varying relative phase was simulated[1]. The signal strength and H-sync timing vary with phase variation from -180 to 180 degrees as shown in Figure 10. H-sync timing varies with or opposite to the signal fading depending on whether the DU ratio has a positive or negative value. In particular, in the case of the negative DU ratio (-7dB) the H-sync timing does not take the values from 0 to 1.3 μsec for the phase differences in the vicinity of ± 180 degrees. This phenomenon is considered as a kind of abrupt
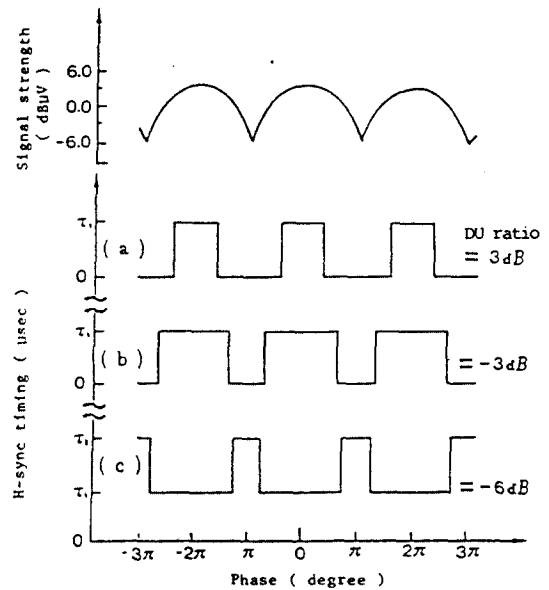

Fig.9 Signal strength and sync timing variation (in case that phase difference varies at constant DU ratio for $\alpha=0.7$).
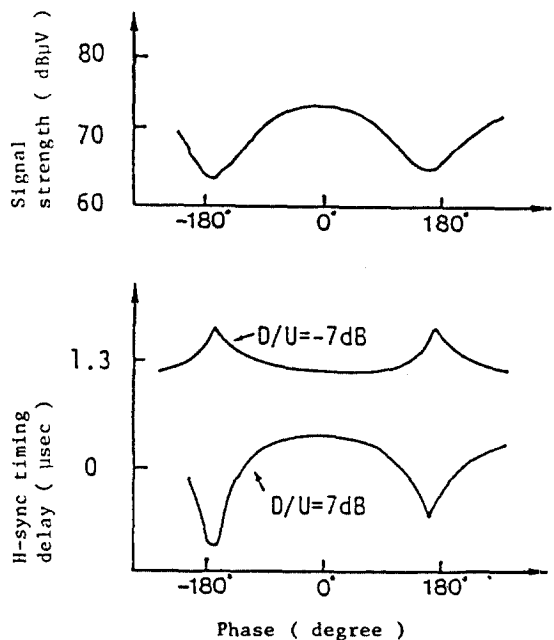

Fig.10 H-sync timing delay vs. phase difference (in case that delay time fixed at 1.3microsecond).

483

variations indicate the loss of synchronization or an unstable synchronization due to the instantaneous disappearence of H-sync signal as affected by frequency-selective deep fade. Also, in the case of the positive DU ratio(7 dB)the H-sync timing takes a lower value than the 0 for the phase difference in the vicinity of ±180 degrees. It can be also considered as a kind of abrupt variations above mentioned. These variation patterns are similar to those of theoretical analysis as shown in Figure 9, however their smoothly varing patterns are not accurately the same as the patterns of theoretical analysis. It is the because that the H-sync pulse, in theoretical analysis, was assumed to be an ideal rectangular wave and the operation of Nyquist filtering and evelope detection were omitted for simplicity.

It can be also considered that when the DU ratio and phase difference vary at random due to multipath interference in the independent Rayleigh-distributed two-ray model (i.e., the vehicle is in motion in an urban area), the H-sync timing fluctuates in conjunction with the received signal strength. Figure 8 will be helpful in understanding why the H-sync timing varies randomly when the DU ratio and phase vary randomly, and Figure 8,9 will be helpful in understanding why the H-sync timing varies with or oppositive to the signal fading when the relative phase difference varies solely at the constant DU ratio.

VI. Conclusions

To investigate the occurrence structure of fluttering ghost the H-sync timing fluctuations was analysed in relation to the multipath parameters, assuming the two-ray propagation model. Relations between the multipath parameters and the variations of the H-sync pulse timing were analysed.

The received H-sync pulse waveform resulting from interference of the multipath waves is distorted. Therfore, the regenerated H-sync timing pulses take on many time values depending on the multipath parameters, and thus fluttering ghost occurs. From the theoretical analysis, it was found that the variations of H-sync pulse timing are directly dependent on the multipath propagation.

REFERENCES

1. T.Takeuchi, D.H.Ha, F.Ikegami, S.Yoshida: "Picture Impairments Due to Multipath Propagation in Mobile TV Reception", IEEE EMC Inter. Sympo. EMC'84 Tokyo, Vol.2. pp.697-701, Oct. 1984.

2. Donald C. Cox and Robert P.Leck: "Correlation Bandwidth and Delay Spread Multipath Propagation Statistics for 910-MHz Urban Mobile Radio Channels", IEEE Trans. on Communications, Vol. Com-23, No. 11, pp.1271-1280, November 1975.

3. F.Ikegami, S.Yoshida: "Analysis of Multipath Propagation Structure in Urban Mobile Radio Environments", IEEE TRans. Antenna & Propag. Vol.AP-28, No.4, pp.531-537, July 1980.

484

河 德 鎬(Deock Ho HA)　　正會員
1954年 2 月 18日生
1972年 3 月～1979年 2 月：漢陽大學校電
子工學科(工學士)
1982年 4 月～1984年 3 月：日本京都大學
大學院電子工學科
(工學碩士)
1984年 4 月～1987年 3 月：日本京都大學
大學院電子工學科
(工學博士)
1974年 2 月～1976年 11月：空軍服務(Radar整備兵)
1978年 11月～1981年 1 月：(株)金星社 中央研究所 勤務
1987年 3 月～1987年 8 月：日本 (株)松下電器無線研究所 勤務
1987年 9 月～現在：國立釜山水産大學電子工學科 專任講師